D-Type Anti-Ferromagnetic Ground State in $Ca_2Mn_2O_5$ *

Pan Liu(刘盼)[1], Wei-Hua Wang(王维华)[1], Wei-Chao Wang(王卫超)[1,2], Ya-Hui Cheng(程雅慧)[1], Feng Lu(卢峰)[1**], Hui Liu(刘晖)[1**]

[1]*Department of Electronics and Tianjin Key Laboratory of Photo-Electronic Thin Film Device and Technology, Nankai University, Tianjin 300071*

[2]*Department of Material Science and Engineering, the University of Texas at Dallas, Richardson 75080, USA*

(Received 9 October 2016)

We study the electronic and magnetic properties of an oxygen-deficient perovskite $Ca_2Mn_2O_5$ based on the first principle calculations. The calculations show that the ground state of $Ca_2Mn_2O_5$ is a D-type anti-ferromagnetic structure with the anti-ferromagnetic spin coupling along the c-direction. The corresponding electronic structure of the D-type state is investigated, and the results display that $Ca_2Mn_2O_5$ is an insulator with an indirect energy gap of ∼2.08 eV. By the partial density-of-state analysis, the valence band maximum is mainly contributed to by the O-2p orbitals and the conduction band minimum is contributed to by the O-2p and Mn-3d orbitals. Due to the Coulomb repulsion interaction between electrons, the density of state of Mn-3d is pulled to −6−−4.5 eV.

PACS: 71.20.−b, 71.15.Mb, 75.50.Ee DOI: 10.1088/0256-307X/34/2/027101

In the 21st century, one of the major scientific challenges is to develop new efficient and low-cost catalysts for energy production or storage technologies. To date, the best catalyst for oxygen electroncatalysis in the acidic solutions is RuO_2 for the oxygen evolution reaction (OER) and the Pt-alloy for the oxygen reduction reaction (ORR).[1−3] However, the high price and scarce crustal abundance on the earth set limitations on their commercial applications. One of the candidates is perovskite materials, due to their flexibility of physical, chemical, in particular catalytic properties. For example, to the ABO_3-type perovskite structure, the A or B site can be varied and replaced by different metal elements, such as non-precious transition metals.[4−8] The desired physical and chemical properties could be obtained by partial replacement or doping at A or B site. Since the discovery of low cost and highly active $Ba_{0.5}Sr_{0.5}Co_{0.8}Fe_{0.2}O_{3-\delta}$ catalyst,[3] a series of perovskite oxide catalysts suitable for oxygen evolution reaction (OER) and oxygen reduction reaction (ORR) have been investigated, such as $Ca_2Mn_2O_5$, $LaCoO_3$, $LaNiO_3$ and $LaMnO_3$.[3−7] Among various non-precious transition metals at the B site, the Mn-based perovskite oxide catalysts have attracted much attention because of their low cost and rich crystal structures.

To date, numerous Mn-based perovskite oxides have been studied in fields of the electrochemical energy storage and conversion, such as $LaMnO_3$, $LiMn_2O_4$, $CaMnO_3$ and $LiMnPO_4$.[5,6] These materials also show better performance in catalytic and electrochemical respects. Thus it is interesting to fully understand their catalytic mechanism of these Mn-based perovskite oxides and further search new Mn-based perovskite oxide catalysts. Kim *et al.* have found that $Ca_2Mn_2O_5$ is one new electrocatalyst with the oxygen-deficient perovskite structure and higher OER activities.[4] Different from the traditional perovskite $CaMnO_3$, Mn and its coordinated oxygen atoms form a square pyramid crystal field not an octahedral crystal field due to the oxygen-defect site present in the crystal structure. From the valence state, Mn is +3 in the $Ca_2Mn_2O_5$, but +4 in the $CaMnO_3$. So far, very few research studies have explored the electronic and magnetic properties of $Ca_2Mn_2O_5$ compound. In this work, we have performed the first principle electronic structure calculations to clarify that the ground state of $Ca_2Mn_2O_5$ is a D-type anti-ferromagnetic (AFM) structure. This magnetic ground state corresponds to the insulator with an indirect energy gap of ∼2.08 eV.

$Ca_2Mn_2O_5$ belongs to the *Pbam* space group (No. 55), and the unit cell is shown in Fig. 1.[4] The Vienna *ab-initio* simulation package (VASP) was employed in the electronic structure calculations.[9−11] The generalized gradient approximation (GGA) with the Perdew–Burke–Ernzerhof (PBE) exchange-correlation potential was adopted.[12] The energy cutoff of the plane wave was set as 500 eV in all of the calculations, while the k-point mesh was set as $11\times5\times17$ for the nonmagnetic structure and $11\times5\times9$ for the spin-polarized magnetic structure, respectively. In the ionic relaxation, the lattice parameters were optimized by the energy minimization with the

*Supported by the National Basic Research Program of China under Grant No 2014CB931703, the National Natural Science Foundation of China under Grant Nos 11404172, 51101088, and 51171082, and the Fundamental Research Funds for the Central Universities.

**Corresponding author. Email: lufeng@nankai.edu.cn

© 2017 Chinese Physical Society and IOP Publishing Ltd

criteria of 1×10^{-4} eV. The relaxed lattice constants of $a = 5.16$ Å, $b = 10.13$ Å and $c = 3.84$ Å, are in agreement with the experimental lattice parameters, $a = 5.43$ Å, $b = 10.24$ Å, $c = 3.74$ Å.[4] To investigate the electronic structure and ground state of $Ca_2Mn_2O_5$, we have carried out the nonmagnetic and spin-polarized calculations. The unit cell in Fig. 1 is adopted to investigate the nonmagnetic state, while in the calculation of the magnetic states including the ferromagnetic (FM) and AFM states, the $1 \times 1 \times 2$ supercell is adopted.

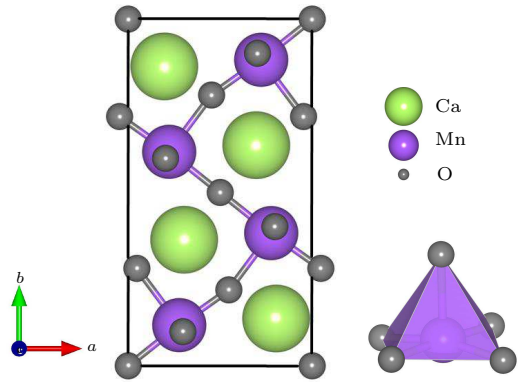

Fig. 1. The crystal structure of oxygen deficient perovskite $Ca_2Mn_2O_5$. Green spheres represent calcium atoms, purple spheres represent manganese atoms and grey spheres represent oxygen atoms. Five oxygen atoms around each manganese atom form a pyramid structure in MnO_5 subunits.

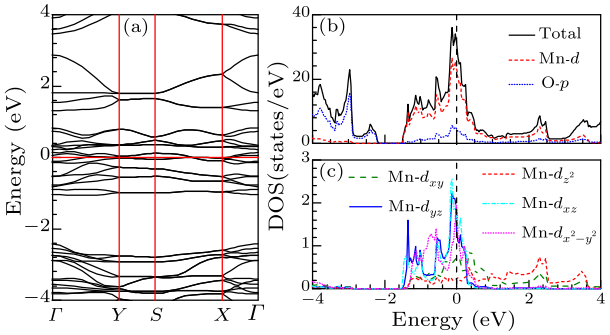

Fig. 2. (a) The band structure of $Ca_2Mn_2O_5$ at the nonmagnetic state, (b) the partial density of states (PDOS) of $Ca_2Mn_2O_5$, and (c) DOS of five Mn-3d orbitals at the nonmagnetic state. The Fermi level is set as zero.

We first present the electronic structures of $Ca_2Mn_2O_5$ in the nonmagnetic state. The corresponding band structure and the density of states (DOS) are shown in Figs 2(a) and 2(b). It is seen that the bands near the Fermi level E_F are very complicated. For example, the energy dispersion is very weak along the high-symmetric Y–S line, indicating a quasi-two-dimensional character. Moreover, several bands cross E_F demonstrating that $Ca_2Mn_2O_5$ is a multi-orbital system. The multi-orbital character can also be found from the DOS. Most of the states near E_F are contributed by the 3d states of Mn, mixing with the O-2p orbitals. As shown in Fig. 2(c), all five Mn-3d orbitals have larger weight near E_F. The contribution of O-2p orbitals is smaller than that from the Mn-3d orbitals. The metal character at the nonmagnetic state is not consistent with the experimental observations since the UV-vis spectroscopy measurement indicates a band gap about 1.35 eV of $Ca_2Mn_2O_5$.[13] It is implied that the on-site electron correlation effect in localized 3d electrons has to be included.

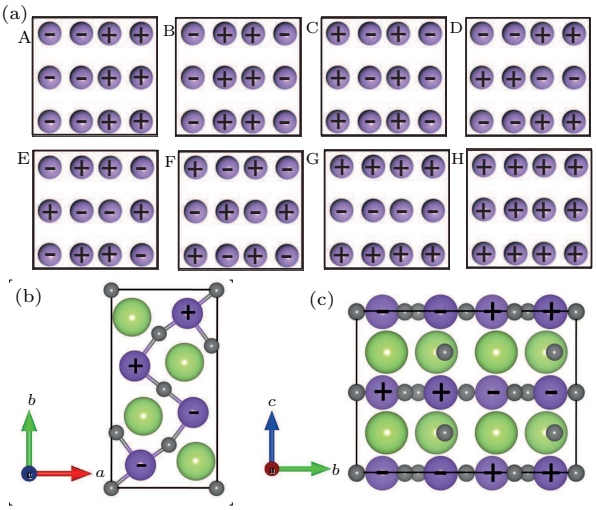

Fig. 3. (a) Eight kinds of magnetic states of $Ca_2Mn_2O_5$ in $1 \times 1 \times 2$ supercell. The positive sign indicates Mn with spin-up localized moment, while the negative sign indicates Mn with spin-down moment. According to the magnetic configurations, eight kinds of states are marked as A-, B-, C-, D-, E-, F-, G- and H-type. (b) The top view of the D-type state. (c) The side view of the D-type state.

To obtain the reasonable ground state of $Ca_2Mn_2O_5$, the spin-polarized magnetic structures are studied with a $1\times1\times2$ supercell. Because the DOS near E_F is mainly contributed by five Mn-3d states, the DFT+U[14] method is used with $U = 5$ eV[15–17] in magnetic structure calculations. By assigning one finite magnetic moment of each Mn atom, all the possible magnetic structures in the quasi-two-dimensional a–b plane are considered. Along the c-axis direction, the FM spin coupling and the AFM spin coupling are also considered, respectively. Generally, eight kinds of magnetic configurations are schematically shown in Fig. 3. A to G are AFM structures, while H is the FM structure. The detailed relative energy and magnetic moment of Mn in these different magnetic structures are listed in Table 1. Among these magnetic states, the energy of D-type AFM state is the lowest, which is the magnetic ground state for $Ca_2Mn_2O_5$. For the D-type AFM state, two parallel ferromagnetic units exist in the a–b plane and they align AFM configuration, while the magnetic moments of Mn keep AFM spin coupling along the c-axis. The energy of the D-type AFM state is lower by 45 meV/Mn than that of the second lowest state-A-type AFM state. In the D-type state, the magnetic moment of Mn is about 3.80 μ_B.

Table 1. The relative energy and magnetic moments of Mn atoms for eight types of magnetic configurations. Here the total energy of D-type is set as the reference energy.

Type	A	B	C	D	E	F	G	H
Relative energy (eV)	0.180	0.902	0.594	0.000	0.714	0.457	0.189	0.409
Magnetic moment of Mn (μ_B)	3.815	3.757	3.749	3.798	3.736	3.731	3.810	3.832

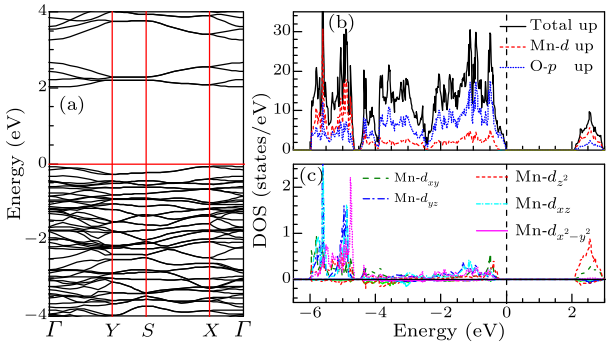

Fig. 4. (a) The electronic band structure of $Ca_2Mn_2O_5$ at the D-type state. The Fermi level is set as zero. The partial density of states of different atoms in (b) and of five Mn-3d orbitals in (c).

The electronic structure of the D-type state is shown in Fig. 4(a). Unlike the metal properties at the nonmagnetic state, the D-type is an insulator with a gap ∼2.08 eV, which is larger than the experimental value. From Fig. 4(a), it is found that the valence band maximum (VBM) is at the line between X and Γ points, while the conduction band minimum (CBM) is at the Γ point. The corresponding DOS is displayed in Fig. 4(b). Different from the DOS contributed by the Mn-3d near E_F in the nonmagnetic state, the PDOS analysis displays that the O-2p orbitals are mainly dominant at the VBM, and the CBM is contributed by both O-2p and Mn-3d orbitals. The PDOS for five Mn-3d orbitals is shown in Fig. 4(c). Obviously, the PDOS of Mn-3d is pushed far away from E_F by the electron–electron Coulomb interaction including intra-orbital and inter-orbital Coulomb interactions. Compared with the nonmagnetic state, it can be seen that PDOS of Mn-3d is distributed in the energy range of −6 eV to −4.5 eV. Moreover, the split e_g orbitals are closer to E_F with respect to the t_{2g} orbitals due to the crystal field effect. As we know, the OH^- prefers to absorb at the oxygen vacant sites on the MnO_5 subunit in the OER catalytic process of $Ca_2Mn_2O_5$.[4] Different from the active sites in metallic catalysts, the OH^- adsorption position is quite unique due to the strong anisotropy of the crystal field in perovskite oxides. For $Ca_2Mn_2O_5$, the adsorbed OH^- has stronger bonding with the Mn-e_g orbitals compared with Mn-t_{2g} orbitals, making $Ca_2Mn_2O_5$ a promising catalyst.

In conclusion, we have presented the electronic structures of $Ca_2Mn_2O_5$ by the first-principles calculation. Our results show that the magnetic ground state of $Ca_2Mn_2O_5$ is a D-type AFM structure. Through analysis of electronic structures, $Ca_2Mn_2O_5$ is an insulator with the indirect band gap of ∼2.08 eV. Based on the PDOS analysis, the VBM is mainly contributed by the O-2p orbitals, and the CBM is contributed by the O-2p and Mn-3d orbitals. Due to the strong Coulomb interaction between 3d electrons, the DOS of Mn-3d is pushed down to −6 eV−−4.5 eV.

References

[1] Lee Y, Suntivich J, May K J, Perry E E and Yang S H 1969 *J. Phys. Chem. Lett.* **3** 399
[2] Stephens I E L, Bondarenko A S, Grønbjerg U, Rossmeisl J and Chorkendorff I 2012 *Energy Environ. Sci.* **5** 6744
[3] Hong W T, Risch M, Stoerzinger K A, Grimaud A, Suntivich J and Yang S H 2015 *Energy Environ. Sci.* **8** 1404
[4] Kim J, Yin X, Tsao K C, Fang S H and Yang H 2014 *J. Am. Chem. Soc.* **136** 14646
[5] Zhang K, Han X P, Hu Z, Zhang X L, Tao Z L and Chen J 2015 *Chem. Soc. Rev.* **44** 699
[6] Suntivich J, Gasteiger H A, Yabuuchi N, Nakanishi H, Goodenough J B and Yang S H 2011 *Nat. Chem.* **3** 546
[7] Suntivich J, May K J, Gasteiger H A, Goodenough J B and Yang S H 2011 *Science* **334** 1383
[8] Tzvetkov P, Kovacheva D, Nihtianova D and Bulgarian T R 2011 *Bulg. Chem. Commun.* **43** 339
[9] Kresse G and Hafner J 1993 *Phys. Rev.* B **47** 558
[10] Kresse G and Hafner J 1994 *Phys. Rev.* B **49** 14251
[11] Kresse G and Farthmüller J 1996 *Phys. Rev.* B **54** 11169
[12] Perdew J P, Burke K and Ernzerhof M 1996 *Phys. Rev. Lett.* **77** 3865
[13] Lu Y, Lu F, Yang Z, Wu J, Yu H, Xie X, Xu J, Cheng F, Chen J, Xiong K, Liu H, Wang W, Zhao J and Wang W 2016 *AIP Adv.* **6** 095210
[14] Dudarev S L, Botton G A, Savrasov S Y, Humphreys C J and Sutton A P 1998 *Phys. Rev.* B **57** 1505
[15] Anisimov V I, Zaanen J and Andersen O K 1991 *Phys. Rev.* B **44** 943
[16] Loschen C, Carrasco J, Neyman K M and Illas F 2007 *Phys. Rev.* B **75** 035115
[17] Lutfalla S, Shapovalov V and Bell A T 2011 *J. Chem. Theory Comput.* **7** 2218